Braced Ductile Shear Panel: New Seismic-Resistant Framing System

Davide Giannuzzi[1]; Roberto Ballarini, P.E., F.ASCE[2]; Arthur Huckelbridge Jr., Dr.Eng., P.E., M.ASCE[3]; Michael Pollino, P.E., A.M.ASCE[4]; and Marco Valente[5]

Introduction

The next-generation seismic lateral force resisting systems (LFRS) should require performance beyond ensuring life-safety and collapse prevention. They should also protect the primary gravity load resisting system by limiting damage to easily replaceable elements so that the structure can be repaired following a major earthquake and remain operational following a moderate earthquake. Limiting or preventing damage to its nonstructural elements and equipment is also desirable from an operational and monetary standpoint (Filiatrault et al. 2001).

To achieve these design objectives, LFRS very often must balance the trade-offs between elastic stiffness (which tends to reduce potential architectural damage by providing enhanced drift control but at the expense of attracting increased seismic loading), strength (which may reduce drift at the expense of increased forces on the surrounding structural members and increased acceleration response of nonstructural components) and ductility (which can limit seismic strength required by providing enhanced energy absorption and dissipation within a specially detailed zone).

Seismic-load resisting systems included in the U.S. code provisions for steel building structures (AISC 2005) vary from traditional moment resisting frames and concentrically and eccentrically braced frames to more recent additions, such as buckling-restrained brace frames and steel plate shear wall systems. Moment resisting frames provide architectural and mechanical flexibility and therefore are an attractive option in design. However, they require ductility within the primary gravity load resisting system (beams and columns), which likely requires significant repair costs following an earthquake to the extent that it may be more cost effective demolish and rebuild.

Seismic bracing has long been a staple of seismic-resistant design since it provides reasonable architectural and mechanical flexibility compared to wall systems and can provide satisfactory performance with a small number of braced frames. Conventional concentrically braced frames (CBFs) [Fig. 1(a)] readily provide high levels of monotonic stiffness and strength. However, they often exhibit strength and stiffness degradation during their plastic cyclic response (Popov et al. 1976; Tremblay 2001). As observed in past earthquake damage (Bertero et al. 1994; AIJ 1997; Nakashima 2000; Bruneau et al. 2011) and in laboratory tests (Khatib et al. 1988; Roeder et al. 2011), CBFs are significantly affected by the poor performance of the braces in compression, occurrence of fracture in the brace after a small number of plastic load reversals, and complicated detailing of the gusset plate connection at the ends of the brace member. Additionally, CBF braces can typically only be arranged in a few configurations and provide few design variables to achieve desirable stiffness, strength, and ductility and design is controlled by compressive brace buckling behavior, all of which

[1]Ph.D. Student, Dept. of Civil Engineering, Univ. of Minnesota, 500 Pillsbury Drive SE, Minneapolis, MN 55455 (corresponding author). E-mail: giann043@umn.edu

[2]James L. Record Professor, Dept. of Civil Engineering, Univ. of Minnesota, 500 Pillsbury Drive SE, Minneapolis, MN 55455.

[3]Professor, Dept. of Civil Engineering, Case Western Reserve Univ., 10900 Euclid Ave., Cleveland, OH 44106-7201. E-mail: aah4@case.edu

[4]Assistant Professor, Dept. of Civil Engineering, Case Western Reserve Univ., Bingham Building, Room 208, 10900 Euclid Ave., Cleveland, OH 44106-7201. E-mail: mcp70@case.edu

[5]Assistant Professor, Dept. of Structural Engineering, Politecnico di Milano, P.za L. Da Vinci 32, 20133 Milano, Italy. E-mail: marco.valente@polimi.it

This manuscript was submitted on July 21, 2012; approved on January 30, 2013; published online on February 1, 2013. Discussion period open until March 8, 2014; separate discussions must be submitted for individual papers

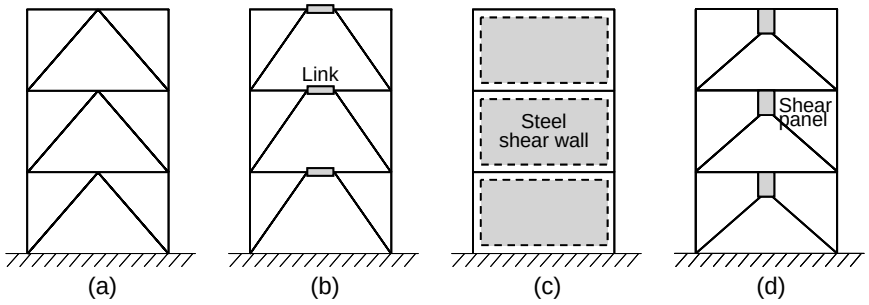

Fig. 1. Seismic load resisting steel systems: (a) concentrically braced frame (CBF); (b) eccentrically braced frame (EBF); (c) steel panel shear wall (SPSW) system; (d) shear panel system

inhibit the potential seismic performance of the lateral system. Properly detailed eccentrically braced frames (EBFs) [Fig. 1(b)] that utilize ductile shear or flexural links placed between eccentric brace connections can provide an attractive combination of strength and ductility (Roeder and Popov 1978; Popov and Engelhardt 1988). The ductile links, however, are relatively complex elements that experience a combination of shear and flexural effects and therefore require careful design treatment (Okazaki et al. 2005). Additionally, the EBF links are currently placed within the gravity load resisting systems (floor beams) and can cause significant damage to the beam and surrounding floor slab that can be costly to repair.

Buckling-restrained braced frames (BRBFs) have similar elastic behavior to CBFs [Fig. 1(a)] with improved plastic performance. The special braces in BRBFs prevent compressive buckling such that the diagonal braces exhibit nearly equal stiffness and strength in tension and compression. In a BRBF, the diagonal braces are encased in a component that restrains buckling of the brace core but does not develop additional force resistance due to friction between the brace core and encasing component. BRBFs were originally developed in Japan after several decades of research and have become a popular structural system worldwide since the late 1990s (Uang and Nakashima 2004). BRBFs overcome many of the shortcomings of CBFs, albeit with substantial cost premium. Additionally, the design parameters to control the systems' lateral stiffness and strength (cross-sectional area and brace length) are somewhat constrained by available bracing configurations (similar to CBFs).

Another important category of seismic load resisting steel systems is the special plate shear wall (SPSW) system shown in Fig. 1(c). SPSWs are a relatively new system whose popularity and attention is growing due to their structural efficiency and ease of construction (Kulak et al. 2001). While this system holds much promise, the behavior of SPSWs is complicated by the complex mode of buckling of the shear wall, associated with tension field action in the shear wall and large forces developed in the beams and columns surrounding the steel wall and must be transmitted into the foundation (Timler and Kulak 1983; Driver et al. 1998). The cyclic plastic behavior of the SPSW system exhibits a significant pinching in the hysteretic response as a result of tension yielding of the infill plate in one direction and limited infill plate resistance under reversed displacement excursion. This displacement needs to overcome inelastic strains from the previous cycle before tension field action yields the plate in the opposite direction (Berman and Bruneau 2005).

Meanwhile, shear panel systems, such as those illustrated in Fig. 1(d) (different configurations are possible), have been used for high-rise buildings in Japan since the 1990s. In many cases, shear panel systems in Japan use low-yield-point-steel (Saeki et al. 1998) to ensure that plastic deformation is strictly contained within the shear panels and the systems are designed to supplement the underlying moment resisting frame. Among currently available systems and systems studied in the past, the shear panel system, shown in Fig. 1(d) most closely resembles the system studied in this work. However, this Japanese system has not been adopted widely in the U.S. practice, perhaps due to the small energy dissipation capacity (as per the use in Japan) or the substantial cost premium.

Past research has also investigated various steel devices that undergo yielding in different modes and can be designed to provide either supplemental passive energy dissipation or the primary lateral force resistance. The added damping and stiffness (ADAS) concept, investigated by Bergman and Goel (1987) and Whittaker et al. (1991), consists of X-shaped steel plates that undergo flexural yielding in double curvature. The similar triangular added damping and stiffness device (TADAS) investigated by Tsai et al. (1993) consists of triangular-shaped steel plates that also undergo flexural yielding but in single curvature. It is often designed to be implemented to the underside of a building beam with a vertical slotted hole to prevent axial forces developing on the triangular plates from gravity loads. Such devices have been shown to provide very ductile hysteretic behavior if proper fabrication tolerances and weld details are achieved. In addition, these devices rely on out-of-plane bracing at the plate end that is not connected to the beam.

While existing LFRS have been developed to satisfy a life safety performance objective, they likely would be difficult to design to achieve desirable seismic performance while providing replaceable ductile components. Seismic steel lateral force resisting systems capable of reduced drift, controllable force capacity, stable hysteretic energy dissipation, and replaceable structural details are needed for the next-generation seismic systems.

Description of the Bracing System

The proposed bracing system consists of concentric X-braces, placed in series with a yielding rectangular ductile shear panel as shown in Fig. 2. Since this system is considered a hybrid of a buckling-restrained braced frame and a steel shear panel system, it is referred to hereafter as the braced ductile shear panel (BDSP) system. The four short I-shaped braces transfer the lateral displacements arising from the lateral load on the building to the shear panel. The ductile shear panel will be comprised of nonslender, in-plane plate elements, stiffened around the perimeter by a boundary flange and capable of achieving high levels of ductility when experiencing plastic shear strains. Unlike the Japanese shear panel systems [the system shown in Fig. 1(d) develops moment at the top and bottom ends which must be transferred into the existing framing], the braced ductile shear panel proposed here is subjected to

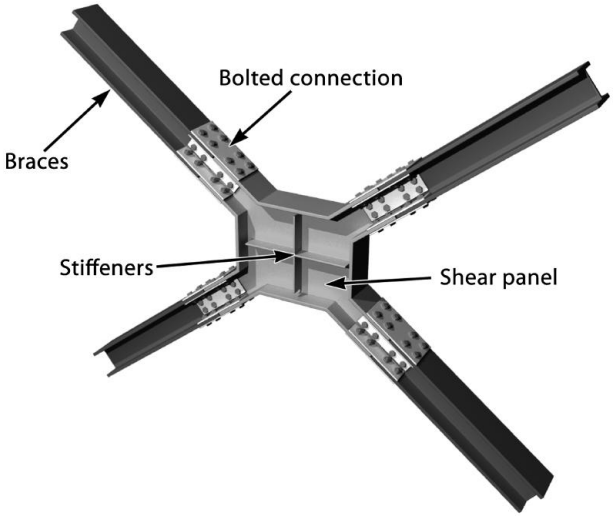

Fig. 2. Braced ductile shear panel

pure shear. Therefore, the behavior of the shear panel is expected to be more stable and reliable (similar to a short EBF link). The braces need not be designed for significant moment, and consequently, capacity design can be more easily and reliably implemented. In addition, the connection between the shear panel and diagonal brace is simplified in the BDSP system. The series configuration ensures that the strength of the ductile shear panel will define the limiting seismic strength demand on the bracing system. The slenderness of the shear panel will be limited such that a stable hysteretic behavior can be ensured for a substantial number of load cycles, even at high levels of ductility demand. It is well known from extensive experimental investigations of eccentrically braced frames, particularly those with shorter length shear links, that cyclic shear yielding can be a stable and dependable mechanism for dissipating seismic energy in a structural system.

Compared to existing steel LFRS, the BDSP is expected to provide benefits of conventional braced frames (reduced drift with reasonable architectural flexibility) but with enhanced energy dissipation capacity and ductility compared to CBF and SPSW, details to allow replacement, and a configuration that provides greater design flexibility to enhance seismic performance.

It is envisioned that the system could be used both in new buildings and as a retrofit measure. The device is also designed so it can be considered sacrificial, meaning that it could be replaced after a severe loading. This implies that the braces and all other elements composing the bracing system other than the BDSP are designed to remain elastic. For the same reason, a bolted connection is required between the braces and the BDSP. Additionally, the connections between the BDSP bracing members and existing framing will primarily be designed for axial force and not require the detailing required for CBF braces (needed to form the buckling brace mechanism). The simplified connection detail would also be beneficial in a seismic rehabilitation by limiting the additional demands placed on the existing framing to axial forces. After an earthquake loading the plastic deformation in the panel will potentially produce large forces in the braces. The question arises how to replace the panel in the presence of these forces. Our preliminary thought is that the bolted connection will most likely be designed as slip-critical to prevent cyclic loading-induced damage to the bolt holes on the beams and will allow free expansion of the braces upon loosening of the bolts in long slotted holes.

Design and Analysis of the Bracing System

Simplified Model and Kinematics

To determine the dimensions, slenderness ratios, and strength of the elements composing the bracing system, it is necessary to understand the behavior of the system prior to and after yielding of the panel.

The aspect ratio of the shear panel a/b is matched to the aspect ratio of the structural frame h/L, so that the shear panel will be in a state of pure shear as long as the braces are able to carry compressive and tensile axial forces to ensure equilibrium.

An estimate of the structural response can be obtained by using a simplified elastic model that captures the basic static and kinematic relationships (Fig. 3). Neglecting the axial deformation in the braces and outer frame, the shearing strain in the panel and the applied shear force can be related to the interstory drift index

$$\gamma = \theta \frac{L}{b} \tag{1}$$

$$V = \tau b t_w = G\gamma b t_w = GLt_w\theta \tag{2}$$

where θ = the rotation of the vertical members; L = the width of the frame; and τ, b, t_w and G = the shear stress, width, thickness, and shear modulus of the sacrificial plate, respectively. The lateral force V is related to the drift index θ through the elastic stiffness of the bracing system, GLt_w as shown in Eq. (2). The simplified model predicts that during elastic response there is no coupling between the in-plane size of the BDSP (dimensions b, a) and the system stiffness.

Finite Element Models

Improved understanding of the local and global structural response is achieved using a three-dimensional geometrically nonlinear

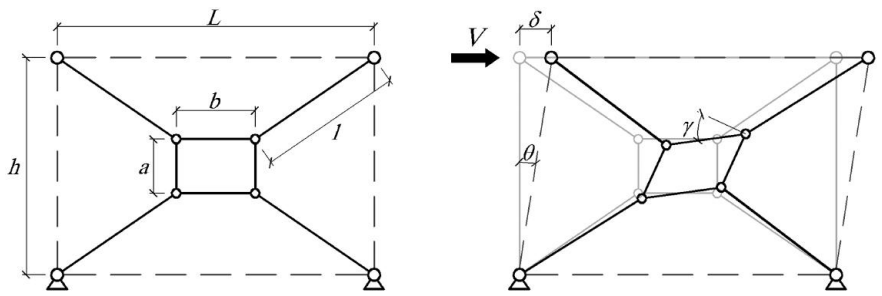

Fig. 3. Simplified model

elastic-plastic (*ABAQUS*) finite-element model. The braces and the BDSP are discretized using shell elements with different elastic-plastic material models used to define the properties of the differing steel grades used in the device and braces.

Braces are modeled as built with steel with yield stress equal to 345 MPa. Since these elements are not expected to experience plastic strains, their constitutive law is assumed to be elastic-perfectly plastic.

The shear panel, however, will undergo large and reversed plastic strains. The simplified elastic-plastic relationship used for the braces would predict inaccurate results by neglecting the strain hardening and the subsequent evolution of the yield surface. In addition, underestimating the maximum stress in the shear panel would lead to a lower capacity demand in the braces, which instead must remain elastic and guarantee enough strength so that the damage is localized in the dissipative device.

It follows that the cyclic behavior of the panel in shear is a fundamental factor to obtain an accurate prediction of the system response. Therefore an elastic-plastic model with nonlinear kinematic and isotropic hardening is assigned to the dissipating elements (Nakashima 1995).

In the material model, the strain rate is decomposed in elastic and plastic components

$$\dot{\varepsilon} = \dot{\varepsilon}^{el} + \dot{\varepsilon}^{pl} \tag{3}$$

The plastic behavior is controlled by the yield function

$$f(\boldsymbol{\sigma} - \boldsymbol{\alpha}) = \sigma^0 \tag{4}$$

where σ^0 is the size of the yield surface, and $\boldsymbol{\sigma}$, α are the stress and backstress tensors, respectively. The yield surface size for isotropic hardening follows the equation:

$$\sigma^0 = \sigma|_0 + Q_\infty(1 - e^{-\kappa\bar{\varepsilon}^{pl}})$$

and the function f is assumed to be von Mises and is written as

$$f(\boldsymbol{\sigma} - \boldsymbol{\alpha}) = \sqrt{\frac{3}{2}(\boldsymbol{\sigma}^{\text{dev}} - \boldsymbol{\alpha}^{\text{dev}}):(\boldsymbol{\sigma}^{\text{dev}} - \boldsymbol{\alpha}^{\text{dev}})} \tag{5}$$

where $\boldsymbol{\sigma}^{\text{dev}}$ = the deviatoric stress tensor; $\boldsymbol{\alpha}^{\text{dev}}$ = the deviatoric part of backstress; and Q_∞ and κ = constants. The flow rule is associated and the rate of plastic flow is defined by the relationship

$$\dot{\bar{\varepsilon}}^{pl} = \frac{\partial f}{\partial \sigma}\sqrt{\frac{2}{3}\dot{\varepsilon}^{pl}:\dot{\varepsilon}^{pl}} \tag{6}$$

The parameters defining the model are fitted to a cyclic stress-strain curve, which models the behavior of structural steel under repeated cyclic loading (Cofie 1985). The resulting yield stress is approximately 240 MPa. Two backstresses are used to define the kinematic hardening in the form

$$\dot{\boldsymbol{\alpha}}_k = \frac{C_k}{\sigma_0}(\boldsymbol{\sigma} - \boldsymbol{\alpha})\dot{\bar{\varepsilon}}^{pl} - \gamma_k\alpha\dot{\bar{\varepsilon}}^{pl} \tag{7}$$

where C_k and γ_k = constants. In Fig. 4, the results from finite element simulation of a cyclic uniaxial tensions-compression specimen are shown, where the values of the fitted parameters are subscripts $C_1 = 24$ GPa, $\gamma_1 = 400$, $C_2 = 1.38$ GPa, $\gamma_2 = 10$, $Q_\infty = 35$ MPa, and $\kappa = 25$.

The boundary conditions are applied at the end of the braces using a rigid constraint on the exterior edges. In the pinned connection models the lower braces are restrained against all displacement and rotations around the horizontal and vertical axes.

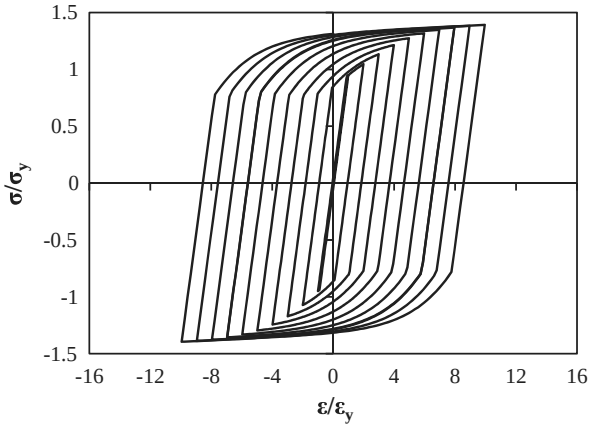

Fig. 4. Calibration of plasticity model

The upper braces have similar restraints except that they are free to move horizontally. The loading, which is applied in the horizontal direction at the upper braces, consists of a unit normal force in the elastic buckling analyses, and a prescribed displacement in the nonlinear cyclic analyses. In the rigid connection models rotations about the axis orthogonal to the bracing system are also restrained.

Elastic Buckling

An estimate of the loads associated with local and global buckling is made using a linearized version of the finite element model. The finite element analyses (not all are presented here because of space limitations) showed that the most critical buckling mode for the geometries and dimensions considered is either the global out-of-plane buckling of two parallel braces about their weak axis or local shear buckling of the BDSP web. Illustrative results for the displacements associated with the latter buckled shape are plotted as contours in Fig. 5 and show that the only part of the structure undergoing significant displacements in this configuration is the shear panel.

Simulations of numerous model geometries suggested that systems that exhibit out-of-plane buckling are associated with decreased stiffness and unsatisfactory performance under cyclic loading. In Fig. 6 the history of the horizontal reaction force at one of the supports (end of brace) is shown for two systems with different dominating buckling mode. Both configurations have an equally wide and thick shear panel ($b = 1{,}000$ mm, $t_w = 7.5$ mm), and therefore are expected to yield at the same load. They also share the same bay width and story height ($L = 4.50$ m, $h = 3.00$ m) and in turn, equal elastic lateral stiffness. The only difference between the models is the section of the braces, which under the assumptions used to derive Eqs. (1) and (2) doesn't affect the lateral elastic stiffness of the system.

In this plot a positive value of the horizontal reaction causes the attaching brace to be tensioned. The brace-buckling dominated system has worse performance in carrying load through the compression brace, and the stiffness degrades with cyclic loading up to the point where the load transferred to the compressive brace is reduced by more than 50%. The total capacity (sum of compression and tension contributions on two symmetric braces) will then also degrade with increasing number of cycles. Note that while AISC suggests a different loading protocol involving cyclic loading at numerous amplitude magnitudes for the purpose of this conceptual design study, a constant amplitude cyclic loading protocol is used.

Therefore, the design of the elements in the bracing system should limit out-of-plane buckling. The only stable post-buckling behavior under cyclic loading is the shear buckling of the shear

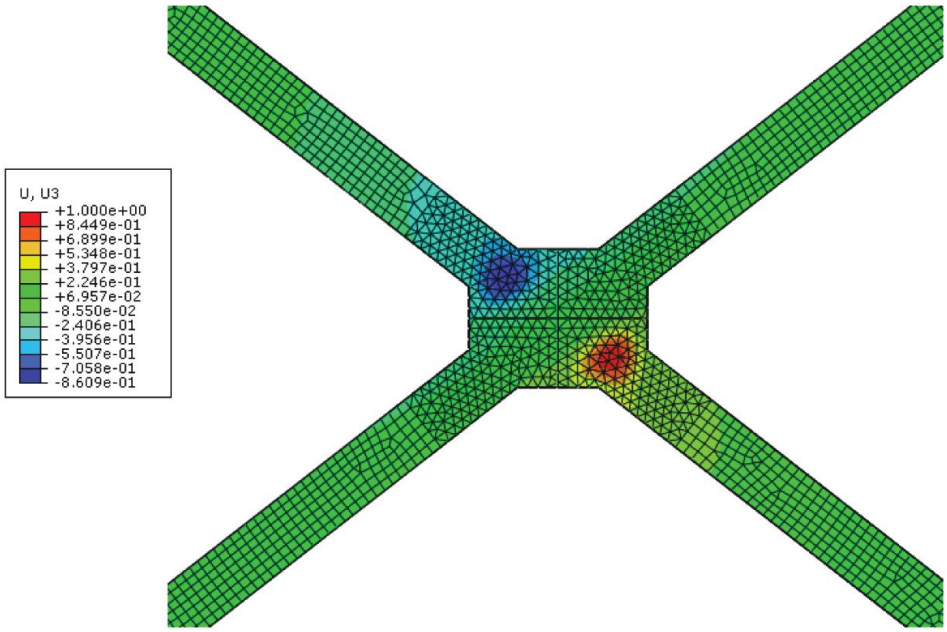

Fig. 5. (Color) Shear buckling of the stiffened BDSP web (contour plot of normalized out-of-plane displacements)

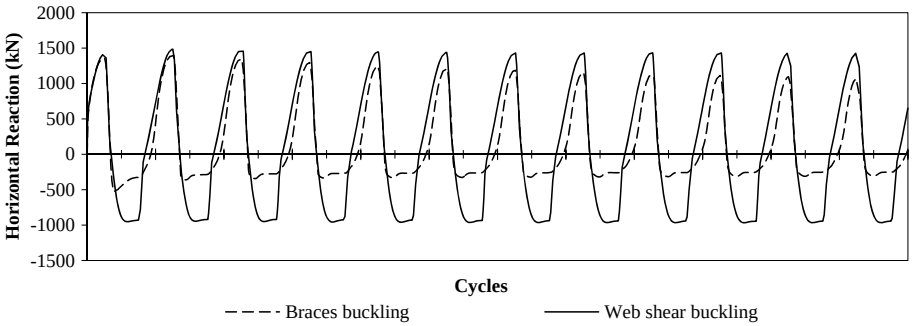

Fig. 6. Comparison of performance for different dominating buckling modes

panel. The following analysis provides insight into the local buckling case.

The critical load for shear buckling of a rectangular plate is equal to

$$F_{sh} = K\pi^2 \frac{D}{a^2} b \tag{8}$$

$$D = \frac{E_s t_w^3}{12(1-\nu^2)} \tag{9}$$

where K is a function of boundary conditions (Bleich 1952)

$$K = \begin{cases} 5.34 + \frac{4.0}{\eta^2} & \text{simply supported plate} \\ 8.98 + \frac{5.6}{\eta^2} & \text{fully restrained plate} \end{cases} \qquad \eta = \frac{b}{a} \geq 1 \tag{10}$$

and b, a, and t_w are the width, height, and thickness of an unstiffened plate (or the in-plane dimensions of the regions that the plate is divided into by stiffeners), respectively, and E_s and ν are the steel's Young's modulus and Poisson ratio.

The shear panel is in a state of uniform shear because $a/b = h/L$. The panel flanges (Fig. 2), as well as the braces, provide partial flexural restraints at the edges of the plate. The critical load is then expected to lie within the buckling load solutions for simply supported and fully restrained plates.

Finite element analyses carried out on models similar to the one described before showed that the critical load for this buckling mode always lies between the loads for the two boundary conditions discussed. In Fig. 7 the buckling loads calculated using Eq. (8) are plotted together with the buckling load from finite elements analyses for 30 different models. The models differ from each other by width and height of the braced frame, thickness, and width of the panel. However, they all share $a/b = h/L$, a vertical and a horizontal stiffener on the shear panel and shear web buckling as the first critical mode. The shear load calculated for the simply supported plate can therefore be used as a lower bound for the critical load. The maximum design load for the bracing system should then be less than the critical load to ensure a stable response and limit the decrease in stiffness of the web due to large transverse displacements.

Nonlinear Analyses

The behavior of the bracing system prior to and after the yielding of the BDSP has been studied using parametric finite elements analyses. All the analyses shared the following features:

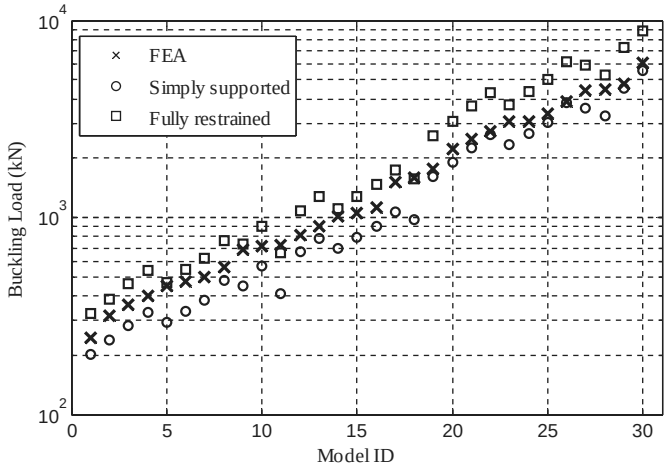

Fig. 7. Buckling loads comparison

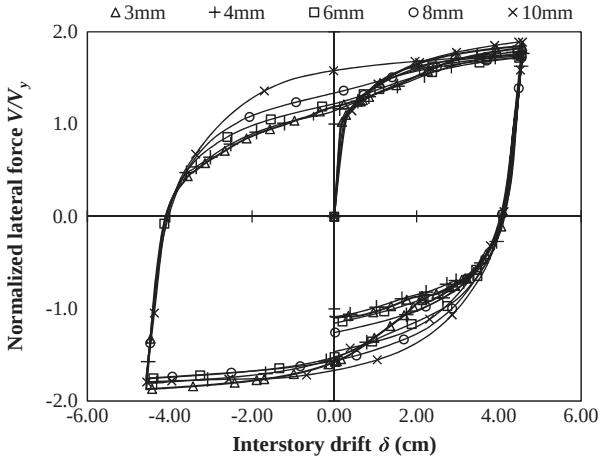

Fig. 8. Normalized force-displacement plot for different panel thicknesses

- Nonlinear geometry and material model (as described earlier).
- 12 fully reversed drift cycles of constant amplitude.
- Amplitude of the cycles to cause a maximum shear strain equal to 0.15.
- Seeded imperfections using the first buckling mode shape.

Parametric studies have been carried out on the following variables:

- BDSP panel thickness (t_w).
- BDSP in-plane size (b, a) with $a/b = h/L$.
- Bay width (L) and story height (h).
- Braces cross-section dimensions.
- Imperfection amplitude (0.25–0.75–2.5 cm).
- Boundary conditions (braces-to-frame connection: *pinned*; *continuous moment*).

The most significant result obtained from the analyses is the curve that relates the applied lateral load V and the displacement δ imposed at the top of the braces. The data showed that Eqs. (1) and (2) are good approximations of the behavior of the system up to the point of yielding. Therefore, they could be used to estimate with sufficient precision the drift and the load that cause first yielding

$$\theta_y = \frac{b}{L}\gamma_y \tag{11}$$

$$\delta_y = \theta_y h \tag{12}$$

$$V_y = GLt_w\theta_y \tag{13}$$

The linear relationship between t_w and V_y can be seen in Fig. 8 where five plots of force-displacement curves for different panel thicknesses are normalized by the load that initiates yielding calculated using Eq. (13); all the normalized curves share the same initial linear segment, and yielding always starts at $V/V_y = 1$, which proves the accuracy of the equation used.

Similarly Eqs. (11) and (12) result in a linear relationship between the interstory drift to cause first yielding and the panel width b, for given constant frame dimensions L and h. Fig. 9 shows three force-displacements curves for varying panel width. The interstory drift δ on the horizontal axis is normalized by the value calculated using Eq. (12). The figure shows that all the plots closely superimpose, that yielding occurs always at $\delta/\delta_y = 1$ and that the yielding load is constant and is independent of the panel width b.

The force-displacement data collected from all the analyses allowed definition of a simple equation to estimate the ultimate load of the bracing system: while neglecting the contribution coming from the flanges surrounding the BDSP web, one can assume that at the ultimate load, the whole shear panel is yielded and reached its maximum shear stress. Therefore the ultimate lateral load will be

$$V_u = \tau_u b t_w \tag{14}$$

These results suggest a bilinear approximation of the force-displacement behavior of a system with given dimensions. The first segment, corresponding to the elastic region, starts at the origin and ends at the point identified by the drift and the lateral load to cause first yielding; the second segment continues from that point to the ultimate drift and load coordinates. The equations used to calculate these points can be solved for the BDSP dimensions, thus allowing the selection of geometries that will result in force-displacement behaviors satisfying practical needs. Note that the panel strength Eq. (14) and stiffness Eq. (13) are decoupled by the panel width design parameter, b, which allows for significant flexibility by the designed to control deformations and limit forces for capacity design. Other current AISC LFRS, such as CBF and BRBF, have limitations on design flexibility.

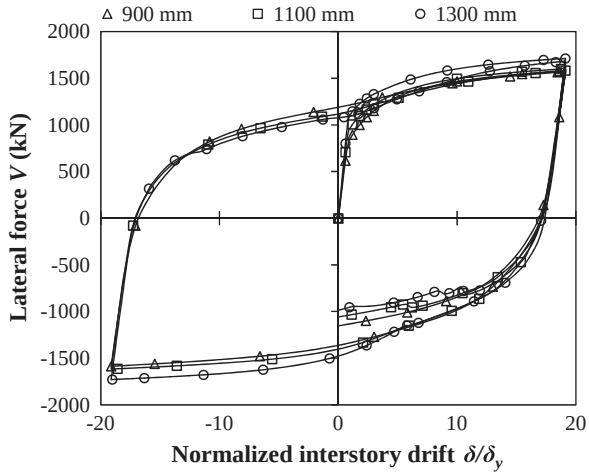

Fig. 9. Normalized force-displacement plot for different panel widths

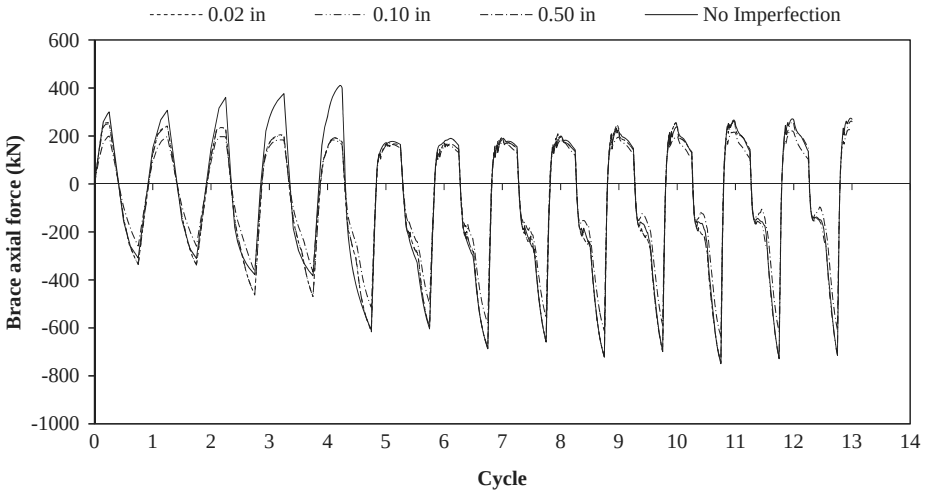

Fig. 10. Axial force in one of the braces under cyclic loading for different initial imperfection amplitudes

The system behavior is not sensitive to imperfection amplitudes as large as 25 mm, which represent extremely large values that significantly exceed acceptable fabrication and erection tolerances. Larger imperfections develop its steady cyclic behavior faster. In fact, under these extreme initial imperfections and cyclic loading, the system tends to displace as the first buckling shape. The amplitude of this deflection initially increases with each load cycle; however, after a few cycles (three to six cycles) this trend ends, and the amplitude stays mostly constant for all subsequent cycles. The imperfections are shown to affect the number of cycles needed to stabilize but not the final response. This behavior can be seen in the plot in Fig. 10, where the axial force in one of the braces under cyclic loading is plotted for different initial imperfection amplitudes (compression if positive). The braces in the model with no imperfections are able to carry more compression in the initial cycles compared to the system with imperfections. However, after a small amount of cycles the responses of the different systems collapse to the same curve.

The force-displacement plots drawn from the analyses showed that the bracing system could achieve a very stable hysteretic behavior. To obtain a stable response, however, special attention must be paid to the slenderness of some key elements. The slenderness of the panel has to be limited so the out-of-plane deformation, caused by the combined effect of imperfections and load reversal, will not affect the in-plane stiffness of the web. This can be achieved (without increasing the thickness of the web and, in turn, the lateral stiffness) with the addition of transverse stiffeners. In addition, the connections and the braces should provide enough flexural stiffness against the out-of-plane buckling to contain the deflection caused by imperfections. The required stiffness for both pinned and fixed end connections would have to be determined for each system. If these issues are not accounted for in the design of the bracing system, the system will undergo cyclic stiffness and strength degradation as a consequence of increasing out-of-plane displacements.

Plastic Dissipation

Another result obtained from the finite element analyses is the proof that the choice of braces section for coupling with a specific panel leads to the concentration of plastic strains only in the BDSP; the braces remain elastic and are thus reusable. Fig. 11 illustrates the evolution of the PEEQ index (equivalent plastic strain) and that no plastic strains are present in the braces throughout the response. The PEEQ index is used as a measure of plastic strains throughout the analysis at each integration point. It is defined as the integral of the absolute value of plastic strain rate; therefore, its value is always greater or equal to zero.

Nonlinear Time-History Analyses on a Steel Frame Equipped with BDSP System

Steel Frame under Study

The effects of the installation of the BDSP device in a steel-framed structure have been studied to estimate the actual benefits provided by the new bracing system. The steel structure under study is a five-bay seven-storey frame. The interstorey height is equal to 3.5 m, and the bay length is equal to 6 m. The steel frame belongs to a building with rectangular plan of 30 × 36 m dimensions consisting of five 6-m bays in the X-direction and six 6-m bays in the Y-direction. Different IPE steel profiles are used for the beams while columns are made of HE320B profiles. The building presents welded connections, and all the elements are made of S355 steel. Fig. 12 shows the plan of the steel building and the elevation of the analyzed frame with the section profiles of beams and columns. The building was designed according to the provisions of Eurocodes 3 and 8, considering a response spectrum type 1, soil type C, and peak ground acceleration $a_g = 0.35$ g. The resulting design spectrum for a return period of 475 years and behavior coefficient $q = 6.0$ is shown in Fig. 13. Dead loads consist of the weights of structural components and partitions, and live loads were considered to be equal to 4 kN/m^2. Storey masses include dead loads and a percentage of live loads (30% according to Eurocode 8 for common residential and office buildings).

Numerical Model of Frame

The steel frame has been numerically modeled using the computer code SAP2000 by means of beam and nonlinear link elements. At each beam and column end, a nonlinear link element has been inserted in the model due to the typical concentration of plasticity at the extremities of the structural elements of MRFs. A schematic view of the insertion of nonlinear link elements at the beam and column ends is shown in Fig. 14.

An elastic-plastic constitutive law is associated to the in-plane rotational degrees of freedom of each link. The generalized

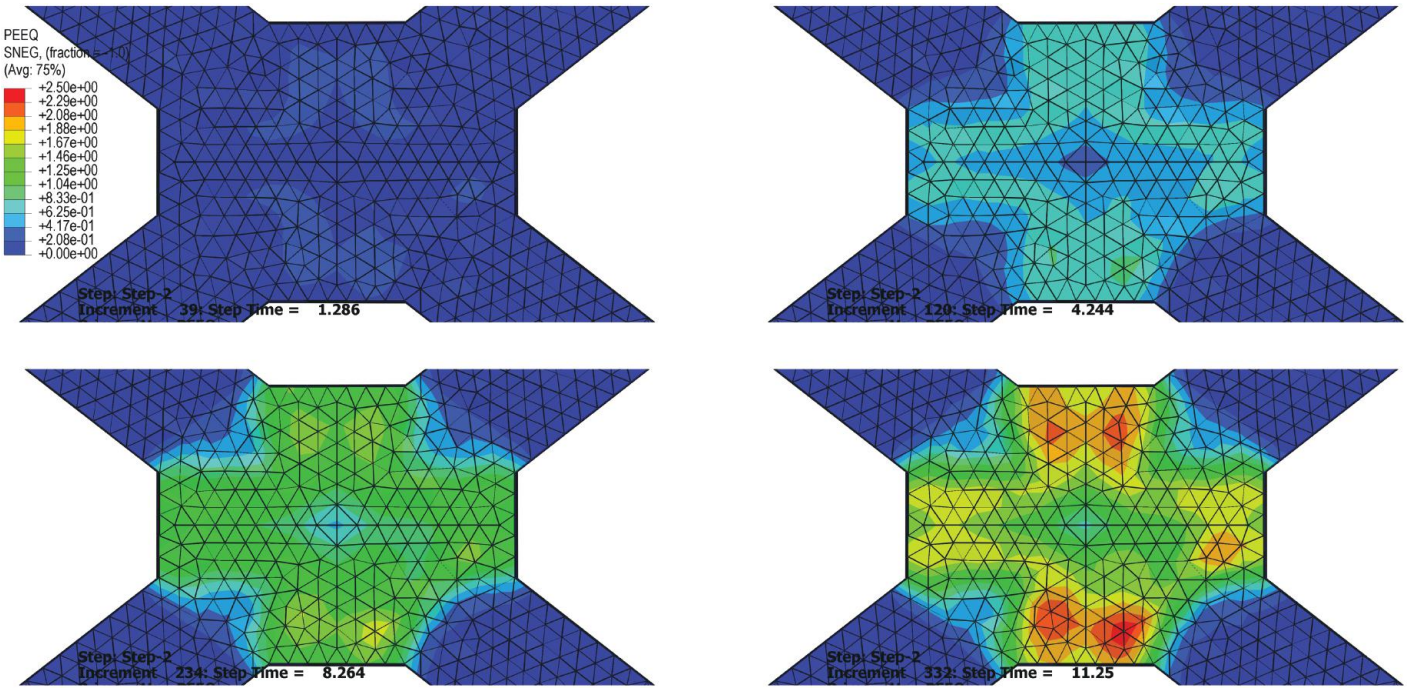

Fig. 11. (Color) Cumulative plastic strain evolution (PEEQ contour plot after 1.25–4.25–8.25–11.25 cycles)

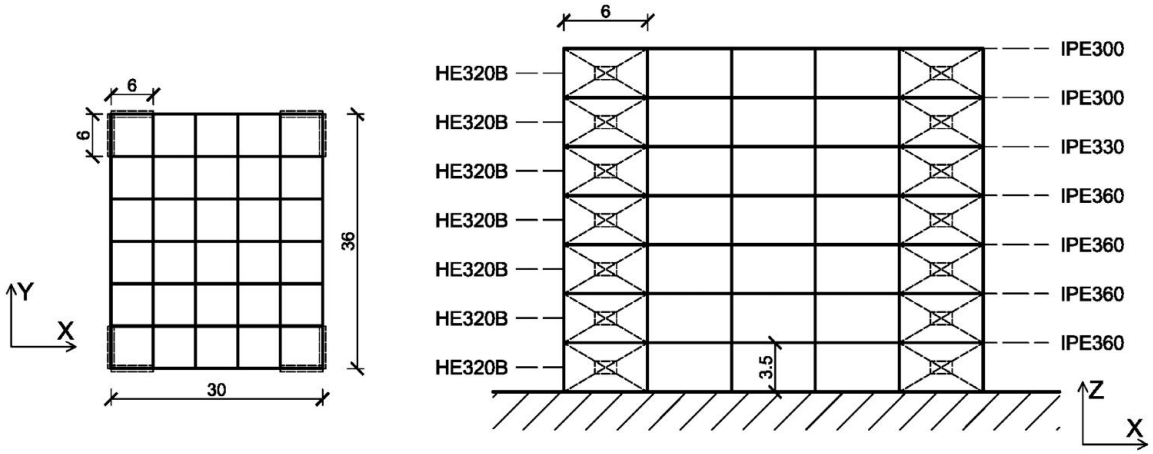

Fig. 12. Building plan and frame elevation (dimensions in m)

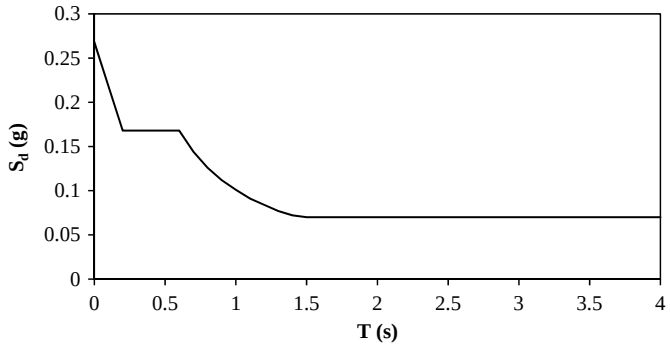

Fig. 13. Design spectrum

force-displacement law used is the Plastic Bouc-Wen model with kinematic hardening (Wen 1976)

$$F = \beta kd + (1-\beta)F_y z \tag{15}$$

where F, d = respectively, the generalized force and displacement for each degree of freedom; k = the linear elastic stiffness; β = the ratio of post-elastic stiffness; F_y = the yielding force; and z = an internal hysteretic variable.

To define the parameters of the model, the yielding bending moments of each beam and column have been calculated. The postelastic stiffness of the curve has been set equal to 0.005 times the elastic stiffness. The length of each link has been assumed equal to the depth of the associated I-shaped element. The numerical

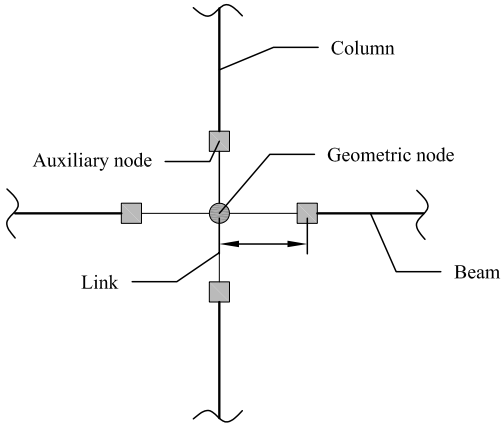

Fig. 14. Plastic hinges model

model allowed for accurately reproducing the seismic response of the frame and to estimate the amount of hysteretic energy dissipated during the seismic excitation.

BDSP-Equivalent Links Model

An equivalent model of the BDSP system has been created to evaluate the effects of the device on the seismic response of the steel frame. Fig. 15 shows the schematic representation of the BDSP model consisting of two link elements crossing the braced bay. The axial degree-of-freedom in each link is associated with an elastic-plastic constitutive law similar to the one used at the extremities of the beam and column elements. However, in this case, the generalized force-displacement curve represents the axial response of each link, and the parameters are calibrated using the expressions for the yielding lateral load and stiffness worked out for the simplified model and verified with the finite element analyses.

The yielding axial force and the elastic stiffness in each link are given by the following expressions:

$$F_y = \frac{V_y}{2\cos\alpha} = \frac{bt_w\tau_y}{2\cos\alpha} \tag{16}$$

$$k = \frac{GLt_w}{2\,h\cos^2\alpha} = \frac{Gt_w}{2\sin\alpha\cos\alpha} \tag{17}$$

where α = the angle between the link and the beam.

The other parameters that control the postyield slope and the sharpness of the curve are fitted to the results obtained from the previous finite element analyses.

The BDSP system was inserted in the lateral bays of all the storeys of the external frames, as shown in Fig. 12.

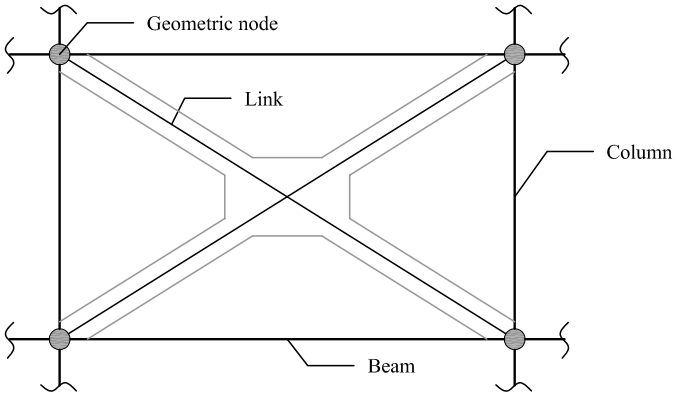

Fig. 15. BDSP-equivalent links model

Numerical Analyses

The El Centro earthquake record (Imperial Valley 1940) with peak ground acceleration scaled to 0.35 g and 0.6 g has been used to perform nonlinear dynamic simulations of the structural response of the steel frame with modal damping equal to 2%. The results obtained from the numerical analyses are reported in terms of top displacement time-history, base shear time-history, and amount of energy dissipated by different mechanisms.

First, a numerical simulation of the seismic response of the MRF has been carried out, and the results obtained in terms of base shear have been used to determine the BDSP parameters (stiffness, yielding load, ultimate load) needed for the design of the device. The first attempt at designing the BDSP is aimed toward protecting the original structure from damage. This objective is then translated into two specific requirements. First, the bracing system should not be designed to resist a lateral force larger than the capacity of the columns and beams. Equilibrium of the axial force in the braces requires additional axial load to be transferred to one adjacent column and beams, which have to be verified under the new loads. This requirement gives a first estimation of the yielding load to aim for in the BDSP design. Second, the interstory drift should be contained so that no plastic deformations are experienced by beams or columns. This second requirement deals with the lateral stiffness of the bracing, thus giving an indication on the thickness of the shear panel.

Then the frame has been provided with the BDSP devices in the lateral bays. In this case the mass pertinent to the frame has been increased since all the seismic force is assumed to be resisted only by the two braced XZ-frames, while in the previous case all the XZ-parallel frames were assumed to participate equally.

The sizes of the devices at different levels have been optimized such that stiffness and strength decrease with the height of the frame, following the shear distribution along the frame. The main objective of the design is to preserve the original structural elements from damage. The characteristics of the BDSP devices inserted at the different levels of the frame are reported in Table 1. The four short braces in the BDSP system consists of HEB280A section profile with S355 steel.

Results and Comparisons

As expected, the presence of the BDSP devices decreased the lateral displacements at the top of the frame. The maximum drift obtained for the BDSP frame is equal to 8.8 cm, while the maximum drift computed for the MRF is equal to 28.3 cm, as shown in Fig. 16.

Fig. 17 indicates that the maximum base shear registered for the BDSP-braced frame (about 1,700 kN) is greater than the one obtained for the MRF (about 1,000 kN). It should be considered that the tributary masses to each BDSP-equipped frame are much larger than the mass tributary to each MRF.

The most relevant effect of the BDSP system on the structural response of the steel frame is in terms of energy dissipation. Fig. 18 shows the amount of energy (normalized with respect to

Table 1. Characteristics of BDSP Device at Different Levels of Frame

Level	$b \times a$ (mm)	t_w (mm)	V_y (kN)
1	1,000 × 583	4	554
2	900 × 525	4	498
3	900 × 525	4	498
4	900 × 525	4	498
5	900 × 525	4	498
6	900 × 525	3	374
7	900 × 525	3	374

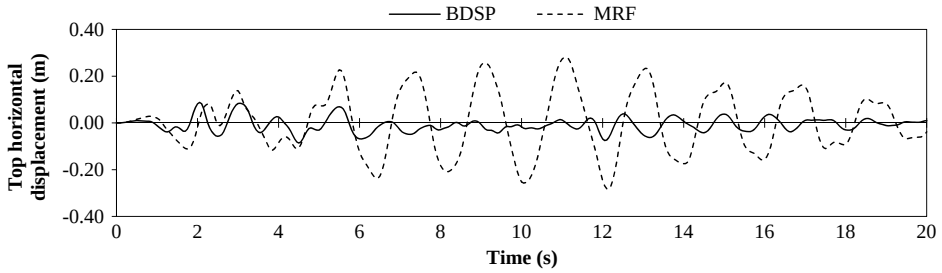

Fig. 16. Top displacement time-history for the two frames under seismic intensity levels equal to $a_g = 0.35$ g

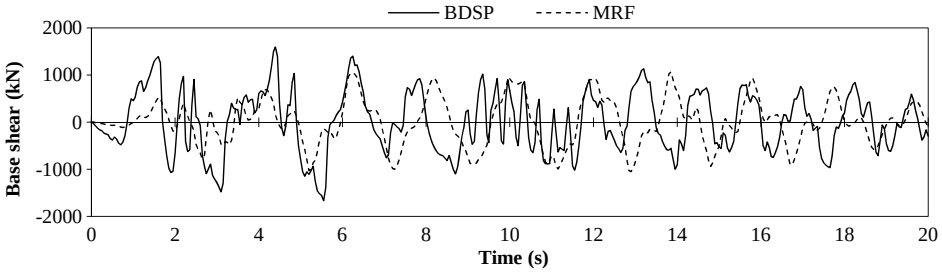

Fig. 17. Base shear time-history for the two frames under seismic intensity levels equal to $a_g = 0.35$ g

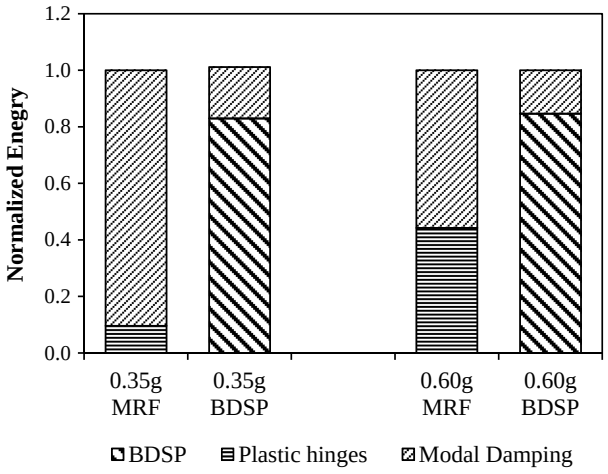

Fig. 18. Amount of energy (normalized with respect to the total dissipated energy) dissipated by different mechanisms in the two frames for different seismic intensity levels

the total input energy) dissipated by the two frames for two different seismic intensity levels. For peak ground acceleration equal to 0.35 g, most of the energy in the MRF is dissipated by modal damping, while only few beams dissipate a small amount of energy. When the peak ground acceleration increases to 0.6 g, the amount of hysteretic energy dissipated at the extremities of the beams is comparable to the one dissipated by modal damping. It's worth noticing that the design of the frame carried out according to Eurocode 8 actually restricts the formation of plastic hinges only to beams, while columns do not experience plastic deformations.

Energy dissipation in the BDSP-equipped frame proved to be much more efficient. For a peak ground acceleration equal to 0.35 g, the devices are able to dissipate a significant amount of energy. At the same time, smaller interstory drifts prevent the formation of plastic hinges in the beams, therefore making the bracing system the only dissipating mechanism besides modal damping. A similar response is obtained in case of excitation with peak ground acceleration of 0.6 g, where most of the energy is dissipated in the bracing system and no plastic hinges occur at the extremities of the beams.

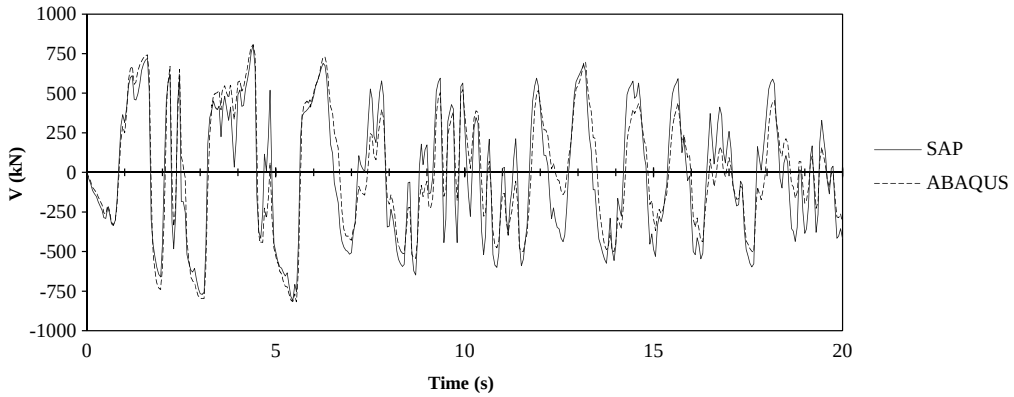

Fig. 19. Lateral force in the bracing system for detailed and reduced model

Validation of Equivalent Link Model

To validate the two links model used to embed the response of the BDSP system in the frame, a detailed model of the system has been created reflecting the dimensions of the one modeled in the frame.

The interstory drift time-history from the dynamic analysis with peak ground acceleration set to 0.60 g is used to prescribe the displacement in the detailed model, and the resulting reaction forces are compared to the shear force predicted in the frame. The plots of the total lateral force against time for both the detailed and reduced model are shown in Fig. 19. The reduced model gives a good approximation of the system response and can therefore be used in a frame analysis to represent the effect of the studied system.

Conclusions and Future Work

The computational study on the new bracing system allowed understanding of the behavior of the ductile panel under cyclic loading. Suggestions have been defined for its design, in particular the slenderness of the elements required to prevent buckling.

The expression for the yielding and ultimate load and the yielding drift index, worked out from the simplified elastic-plastic model, has been proven to be accurate in describing the global response of the bracing system and has been successfully used to model the BDSP in a framed structure. The BDSP was shown to provide stable hysteretic behavior and design parameters that can enhance system performance compared to other steel LFRS. It is capable of undergoing significant plastic deformations without causing damage to surrounding framing and can be replaced following an earthquake.

The dynamic analyses on the 2D frame showed that the installation of the bracing system in a steel structure would provide several benefits to the structural response, most important being an increase in ductility and the possibility to prevent large plastic zones in other structural elements, such as floor beams.

Future developments for the numerical model will be aimed at calibrating the finite element model to experimental results. This could include also the addition of a damage/failure criterion to predict the ductile failure of the steel panel.

Experimental tests are required and currently being planned to assess the potential of the BDSP, to validate the computational simulation results, and to address the design detailing requirements, which will play crucial roles in the system's performance. To this extent the possibility of applying the AISC seismic provisions for detailing of EBF links to the BDSP system will also be investigated.

References

American Institute of Steel Construction (AISC). (2005). *Seismic Provisions for Structural Steel Buildings*, Chicago.

Architectural Institute of Japan (AIJ). (1997). "Reconnaissance report on damage to steel building structures observed from the 1995 Hyogoken-Nanbu (Hanshin/Awaji) earthquake." Kinki Branch, AIJ, Osaka, Japan.

Bergman, D. M., and Goel, S. C. (1987). "Evaluation of cyclic testing of steel-plate devices for added damping and stiffness." *Rep. UMCE 87-10*, Civil Engineering Dept., Univ. of Michigan, Ann Arbor, MI.

Berman, J., and Bruneau, M. (2005). "Experimental investigation of light-gauge steel plate shear walls." *J. Struct. Eng.*, 10.1061/(ASCE)0733-9445(2005)131:2(259), 259–267.

Bertero, V. V., Anderson, J. C., and Krawinkler, H. (1994). "Performance of steel building structures during the Northridge earthquake." *EERC-94/09*, Univ. of Berkley, Berkley, CA.

Bleich, F. (1952). *Buckling strength of metal structures*, McGraw Hill, New York.

Bruneau, M., Uang, C. M., and Sabelli, R. (2011). *Ductile design of steel structures*, 2nd Ed., McGraw Hill, New York.

Cofie, N. G., and Krawinkler, H. (1985). "Uniaxial cyclic stress-strain behavior of structural steel." *J. Eng. Mech.*, 10.1061/(ASCE)0733-9399(1985)111:9(1105), 1105–1120.

Driver, R. G., Kulak, G. L., Kennedy, D. J. L., and Elwi, A. E. (1998). "Cyclic test of four-story steel plate shear wall." *J. Struct. Eng.*, 10.1061/(ASCE)0733-9445(1998)124:2(112), 112–130.

Filiatrault, A., Uang, C. M., Folz, B., Christopoulos, C., and Gatto, K. (2001). "Reconnaissance report of the February 28, 2011 nisqually (Seattle-Olympia) earthquake." *Structural Systems Research Project Rep. No. SSRP-2000/15*, Dept. of Structural Engineering, Univ. of California, San Diego, La Jolla, CA.

Khatib, I. F., Mahin, S. A., and Pister, K. (1988). "Seismic behavior of concentrically braced steel frames." *EERC-88/01*, Univ. of California, Berkley, CA.

Kulak, G. L., Kennedy, D. J. L., Driver, R. G., and Medhekar, M. (2001). "Steel plate shear walls: An overview." *Eng. J.*, 38(1), 50–62.

Nakashima, M. (1995). "Strain-hardening behavior of shear panels made of low-yield steel. I: Test." *J. Struct. Eng.*, 10.1061/(ASCE)0733-9445(1995)121:12(1742), 1742–1749.

Nakashima, M. (2000). "Overview of damage to steel building structures observed in the 1995 Kobe earthquake." *FEMA-355E State of the art Rep. on past performance of steel moment-frame buildings in earthquakes*, Federal Emergency Management Agency, Washington, DC.

Okazaki, T., Arce, G., Ryu, H. C., and Engelhardt, M. D. (2005). "Experimental study of local buckling, overstrength and fracture of links in eccentrically braced frames." *J. Struct. Eng.*, 10.1061/(ASCE)0733-9445(2005)131:10(1526), 1526–1535.

Popov, E. P., and Engelhardt, M. D. (1988). "Seismic eccentrically braced frames." *J. Constr. Steel Res.*, 10, 321–354.

Popov, E. P., Takanashi, K., and Roeder, C. W. (1976). "Structural steel bracing systems." *EERC Rep. 76-17*, Univ. of California, Berkeley, CA.

Roeder, C. W., et al. (2011). "Influence of gusset plate connection and braces on the seismic performance of X-braced frames." *Earthquake Eng. Struct. Dynam.*, 40(4), 355–374.

Roeder, C. W., and Popov, E. P. (1978). "Cyclic shear yielding of wide-flange beams." *Eng. Mech.*, 104(4), 763–780.

Saeki, E., Sugisawa, M., Yamaguchi, T., and Wada, A. (1998). "Mechanical properties of low yield point steels." *J. Mater. Civ. Eng.*, 10.1061/(ASCE)0899-1561(1998)10:3(143), 143–152.

Timler, P. A., and Kulak, G. L. (1983). "Experimental study of steel plate shear walls." *Structural Engineering Rep. No. 114*, Dept. of Civil Engineering, Univ. of Alberta, Edmonton, AB, Canada.

Tremblay, R. (2001). "Seismic behaviour and design of concentrically braced steel frames." *Eng. J.*, 38(3), 148–166.

Tsai, K. C., Chen, H. W., Hong, C. P., and Su, Y. F. (1993). "Design of steel triangular plate energy absorbers for seismic-resistant construction." *Earthquake Spectra*, 9(3), 505–528.

Uang, C. M., and Nakashima, M. (2004). "Steel buckling-restrained braced frames." Chapter 16, *Earthquake engineering: From engineering seismology to performance-based engineering*, Y. Bozorgnia and V. V. Bertero, eds., CRC Press, Boca Raton, FL, 16-1–16-37.

Wen, Y. K. (1976). "Method for random vibration of hysteretic systems." *J. Engrg. Mech. Div.*, 102(2), 249–263.

Whittaker, A. S., Bertero, V. V., Thompson, C. L., and Alonso, L. J. (1991). "Seismic testing of steel plate energy dissipation devices." *Earthquake Spectra*, 7(4), 563–604.